Contemporary Mathematics
https://ojs.wiserpub.com/index.php/CM/

Research Article

Stochastic Dynamics in Multi-Population Epidemic Models: Unveiling Noise-Induced Variability and Stability

Shah Hussain[1*], **Thoraya N. Alharthi**[2]

[1]Department of Mathematics, College of Science, University of Hail, Hail, 2440, Saudi Arabia
[2]Department of Mathematics, College of Science, University of Bisha, P.O. Box 551, Bisha, 61922, Saudi Arabia
E-mail: s.khan@uoh.edu.sa

Received: 5 August 2025; **Revised:** 25 September 2025; **Accepted:** 10 October 2025

Abstract: This paper investigates the stochastic dynamics of a multi-population epidemiological model using the Milstein method to discretize the governing equations. The model incorporates susceptible, infected, hospitalized, and recovered populations, with noise intensities influencing the transmission dynamics. In the deterministic case, the system exhibits smooth and predictable behavior, with populations converging to equilibrium values. However, the introduction of stochastic noise leads to significant variability in the system dynamics. Low noise intensities result in minimal fluctuations, while high noise levels induce pronounced and extreme stochastic behavior. The infected population is particularly sensitive to noise, with high noise intensities causing destabilization. These findings highlight the critical role of noise in epidemiological modeling and underscore the importance of controlling stochastic effects to maintain system stability.

Keywords: disease persistence, disease extinction, stability

MSC: 34D20, 47A35, 60H10

1. Introduction

Epidemic modeling is an important foundation for understanding transmission dynamics and guiding public health interventions. Deterministic frameworks have yielded foundational insights, but do not represent the intrinsic randomness of real outbreaks, arising from environmental fluctuations, contact heterogeneity, and behavioral variability. Historical accounts of influenza pandemics of the 20th and 20th centuries underscore how context and variability shape the burden of the disease [1–3]. Building on this context, recent statistical and virological syntheses consolidate modern evidence on transmission, inference, and antiviral resistance, reinforcing the need for models that explicitly encode heterogeneity and stochastic drivers [4–6].

Consequently, contemporary work integrates stochastic processes to capture extinction-persistence trade-offs and noise-induced variability. For example, a stochastic Susceptible-Exposed-Infectious-Quarantined-Recovered-eXtra (SEIQRX) framework with generalized incidence and Lyapunov analysis establishes global positivity and clarifies the conditions for long-term extinction or persistence under random perturbations [7]. Models incorporating awareness decay and individual heterogeneity on multi-weighted networks show how fluctuations in both infection and awareness channels shape thresholds and outcomes [8]. Hierarchical and multiphasic stochastic formulations, with piecewise

DOI: https://doi.org/10.37256/cm.6520258147

constant transmission that captures distinct epidemic stages, further illuminate how environmental variability and contact structure modulate dynamics across phases [9, 10].

Complementing these structural views, seasonality remains a key modulator of transmission and is commonly incorporated through periodic or data-driven terms to sharpen prediction and intervention design [11, 12].

1.1 *Research gap and novelty*

While stochastic epidemic models are well studied, many works either (i) treat a single susceptible class or (ii) do not explicitly separate *state-dependent* (multiplicative) variability that scales with contacts from other sources of noise. Real-world epidemics feature heterogeneity in risk between subpopulations and variability driven by interaction in transmission. This study addresses these gaps by formulating a model with two susceptible groups and *multiplicative* environmental noise acting on incidence, which preserves positivity and reflects the empirically observed increase in variability when prevalence and susceptibility are high. The novelty of this work lies in [13–15].

• Explicitly modeling two distinct susceptible populations ($\mathcal{S}_1$ and $\mathcal{S}_2$) to represent heterogeneous risk.

• Using *multiplicative* (state-dependent) noise on transmission, consistent with interaction-driven uncertainty and the positivity-preserving analysis carried out in the paper.

• Deriving sharp, interpretable conditions for extinction and persistence in terms of a stochastic threshold $\mathcal{R}_0^S$, together with long-time martingale limits.

Building upon these developments, the current study introduces a stochastic epidemic model that incorporates environmental noise into a deterministic framework. The primary contributions include the following.

• Establishing global existence, non-explosion, and positivity of solutions via a Lyapunov/stopping-time argument on $\mathbb{R}^5_+$.

• Deriving an extinction criterion: if $\mathcal{R}_0^S < 1$ with $\mathcal{R}_0^S = \dfrac{\dfrac{\beta_1\Lambda_1+\beta_2\Lambda_2}{\alpha} - \dfrac{1}{2}\left(\eta_1^2\dfrac{\Lambda_1^2}{\alpha^2} + \eta_2^2\dfrac{\Lambda_2^2}{\alpha^2}\right)}{\mu+\alpha}$, then $\mathcal{I}(t)$ decays exponentially almost surely.

• Proving persistence when $\mathcal{R}_0^S > 1$ (and obtaining explicit lower bounds under a mild mean-field closure for time averages).

• Providing simulations (Euler-Maruyama) that validate the theoretical thresholds and illustrate how increasing noise intensities (η_1, η_2) amplify variability in epidemic trajectories.

Together, these results clarify how risk heterogeneity and multiplicative environmental variability shape epidemic outcomes, bridging rigorous long-time analysis with numerically observed behavior, and complementing recent developments in the literature [16–20].

2. Model formulation

Epidemic dynamics are inherently influenced by environmental and demographic randomness. To capture these uncertainties, we introduce stochastic perturbations into key epidemiological parameters using additive noise, which represents external random fluctuations independent of population size. These fluctuations arise from unpredictable factors such as seasonal variations, healthcare infrastructure efficiency, and policy changes.

2.1 *Stochastic epidemic model (multiplicative noise)*

The Stochastic Differential Equations (SDEs) governing the epidemic dynamics are:

$$d\mathcal{S}_1 = \big(\Lambda_1 - \beta_1\mathcal{I}\mathcal{S}_1 - \alpha\mathcal{S}_1\big)dt - \eta_1\mathcal{I}\mathcal{S}_1 d\mathcal{W}_1,$$

$$d\mathcal{S}_2 = \big(\Lambda_2 - \beta_2 \mathcal{I}\mathcal{S}_2 - \alpha \mathcal{S}_2\big)dt - \eta_2 \mathcal{I}\mathcal{S}_2 d\mathscr{W}_2,$$

$$d\mathcal{I} = \big(\mathcal{I}(\beta_1 \mathcal{S}_1 + \beta_2 \mathcal{S}_2) - (\mu + \alpha)\mathcal{I}\big)dt + \eta_1 \mathcal{I}\mathcal{S}_1 d\mathscr{W}_1 + \eta_2 \mathcal{I}\mathcal{S}_2 d\mathscr{W}_2,$$

$$d\mathcal{H} = \big(\mu \mathcal{I} - (\rho + \alpha)\mathcal{H}\big)dt,$$

$$d\mathcal{R} = \big(\rho \mathcal{H} - \alpha \mathcal{R}\big)dt. \tag{1}$$

Here, $d\mathscr{W}_1$ and $d\mathscr{W}_2$ are independent Brownian motions, and η_1 and η_2 denote the intensities of stochastic fluctuations. We adopt *multiplicative* (state-dependent) noise: the diffusion terms $\eta_1 \mathcal{I}\mathcal{S}_1\, d\mathscr{W}_1$ and $\eta_2 \mathcal{I}\mathcal{S}_2\, d\mathscr{W}_2$ scale with interaction rates, which is standard for epidemic transmission modeling [21]. Unlike additive (state-independent) noise, multiplicative noise captures the empirically observed increase in variability when $\mathcal{I}$ and $\mathcal{S}_i$ are large.

2.1.1 *Choice of multiplicative noise*

This choice reflects the assumption that environmental fluctuations primarily modulate effective contacts/transmission, so variability grows with the state. While additive noise can represent exogenous shocks independent of population size, the present SDEs already employ state-dependent diffusion consistent with interaction-driven uncertainty [22].

2.2 *Model components and parameters*

The system consists of five epidemiological compartments:
- $\mathcal{S}_1$: Susceptible individuals with no underlying health conditions.
- $\mathcal{S}_2$: Susceptible individuals with higher risk due to age or pre-existing health conditions.
- $\mathcal{I}$: Infected individuals.
- $\mathcal{H}$: Individuals receiving treatment.
- $\mathcal{R}$: Recovered individuals.

The parameters of the model are:
- Λ_1: Influx rate of the susceptible class $\mathcal{S}_1$.
- Λ_2: Influx rate of the susceptible class $\mathcal{S}_2$.
- α: Natural death rate of the human population.
- β_1: Infection rate between susceptible class $\mathcal{S}_1$ and the infected population.
- β_2: Infection rate between susceptible class $\mathcal{S}_2$ and the infected population.
- μ: Treatment rate of infected individuals.
- ρ: Recovery rate from infection.

Splitting susceptibility into $(\mathcal{S}_1,\ \mathcal{S}_2)$ captures risk heterogeneity (e.g., comorbidity/age strata) and aligns with intervention design (targeted shielding or prioritization), while preserving the tractability of the transmission terms.

2.3 *Feasible region*

Let $\mathcal{N}(t) = \mathcal{S}_1(t) + \mathcal{S}_2(t) + \mathcal{I}(t) + \mathcal{H}(t) + \mathcal{R}(t)$. Summing (1) gives the exact total-population dynamics $d\mathcal{N}(t) = \big(\Lambda_1 + \Lambda_2 - \alpha \mathcal{N}(t)\big)\, dt$, since the stochastic terms cancel. Hence $\mathcal{N}(t) \le \max\big\{\mathcal{N}(0),\ (\Lambda_1 + \Lambda_2)/\alpha\big\}$ for all $t \ge 0$. In particular, the set

$$\Gamma = \left\{ (\mathcal{S}_1(t), \mathcal{S}_2(t), \mathcal{I}(t), \mathcal{H}(t), \mathcal{R}(t)) \in \mathbb{R}^5_+ : \mathcal{N}(t) \leq \frac{\Lambda_1 + \Lambda_2}{\alpha} \right\},$$

is positively invariant for system (1) whenever $\mathcal{N}(0) \leq (\Lambda_1 + \Lambda_2)/\alpha$; more generally, the trajectory enters this set in finite time and remains there thereafter.

2.4 *Reduction to the deterministic model*

When stochastic perturbations are absent ($\eta_1 = \eta_2 = 0$), the system reduces to its deterministic counterpart [17]:

$$\begin{aligned}
\frac{d\mathcal{S}_1}{dt} &= \Lambda_1 - \beta_1 \mathcal{I}\mathcal{S}_1 - \alpha\mathcal{S}_1, \\
\frac{d\mathcal{S}_2}{dt} &= \Lambda_2 - \beta_2 \mathcal{I}\mathcal{S}_2 - \alpha\mathcal{S}_2, \\
\frac{d\mathcal{I}}{dt} &= \mathcal{I}(\beta_1\mathcal{S}_1 + \beta_2\mathcal{S}_2) - (\mu + \alpha)\mathcal{I}, \\
\frac{d\mathcal{H}}{dt} &= \mu\mathcal{I} - (\rho + \alpha)\mathcal{H}, \\
\frac{d\mathcal{R}}{dt} &= \rho\mathcal{H} - \alpha\mathcal{R}.
\end{aligned} \tag{2}$$

2.5 *Significance of stochasticity*

Including stochasticity improves realism by capturing uncertainties that deterministic models cannot. For interaction-driven transmission, *multiplicative* noise is appropriate because variability scales with $\mathcal{I}$ and $\mathcal{S}_i$, consistent with stochastic epidemic modeling practice. This modeling choice provides a robust framework for understanding epidemic behavior under fluctuating environmental and healthcare conditions [23, 24].

3. Preliminaries

To analyze the stochastic epidemic model rigorously, we begin by introducing essential definitions and mathematical preliminaries. These provide the foundational tools necessary for understanding the existence, stability, and long-term behavior of the system.

Definition 3.1 (tochastic Process, [25]) A *stochastic process* is a collection of random variables $\{X(t)\}$, where for each fixed $t \in [0, T]$, $X(t)$ is a random variable defined on a probability space $(\Omega, \mathcal{F}, \mathbb{P})$. A stochastic process is said to be *adapted* to a filtration $\mathbb{F} = \{\mathcal{F}_t\}_{t\geq 0}$ if for each t, the random variable $X(t)$ is measurable with respect to $\mathcal{F}_t$, meaning that all past and present information up to time t is contained in $\mathcal{F}_t$.

Throughout this paper, we work on a complete filtered probability space $(\Omega, \mathcal{F}, \{\mathcal{F}_t\}_{t\geq 0}, \mathbb{P})$ satisfying the usual conditions. The state process $\mathcal{X}(t) = (\mathcal{S}_1, \mathcal{S}_2, \mathcal{I}, \mathcal{H}, \mathcal{R})^\top$ takes values in $\mathbb{R}^5_+$, endowed with its Borel σ-algebra $\mathcal{B}(\mathbb{R}^5_+)$.

3.1 *Stochastic differential equation representation*

The Stochastic Differential Equation (SDE) that governs the dynamics of the epidemic system is formulated as:

$$d\mathcal{X}(t) = H(\mathcal{X}(t))\,dt + G(\mathcal{X}(t))\,d\mathcal{W}(t), \quad t \geq 0, \tag{3}$$

$$\mathcal{X}(0) = \mathcal{X}_0 \in \mathbb{R}^5_+, \tag{4}$$

where $\mathcal{W}(t) = (\mathcal{W}_1(t), \mathcal{W}_2(t))^\top$ is a two-dimensional Brownian motion with independent components, adapted to $\{\mathcal{F}_t\}_{t\geq 0}$. In addition:

• $\mathcal{X}(t) = (\mathcal{S}_1, \mathcal{S}_2, \mathcal{I}, \mathcal{H}, \mathcal{R})^T$ is the state vector representing the system variables at time t.

• The *drift term* $H(\mathcal{X}(t))$ captures the deterministic part of the system:

$$H(\mathcal{X}) = \begin{bmatrix} \Lambda_1 - \beta_1 \mathcal{I}\mathcal{S}_1 - \alpha\mathcal{S}_1 \\ \Lambda_2 - \beta_2 \mathcal{I}\mathcal{S}_2 - \alpha\mathcal{S}_2 \\ \mathcal{I}(\beta_1\mathcal{S}_1 + \beta_2\mathcal{S}_2) - (\mu+\alpha)\mathcal{I} \\ \mu\mathcal{I} - (\rho+\alpha)\mathcal{H} \\ \rho\mathcal{H} - \alpha\mathcal{R} \end{bmatrix}.$$

The drift term $H(\mathcal{X})$ is continuously differentiable and thus locally Lipschitz on $\mathbb{R}^5_+$.

• The *diffusion term* $G(\mathcal{X}(t))$ represents stochastic fluctuations in the system due to random environmental perturbations:

$$G(\mathcal{X}) = \begin{bmatrix} -\eta_1\mathcal{I}\mathcal{S}_1 & 0 \\ 0 & -\eta_2\mathcal{I}\mathcal{S}_2 \\ \eta_1\mathcal{I}\mathcal{S}_1 & \eta_2\mathcal{I}\mathcal{S}_2 \\ 0 & 0 \\ 0 & 0 \end{bmatrix}.$$

• The diffusion exhibits polynomial (not linear) growth; for some $C > 0$,

$$\|G(\mathcal{X})\|_F^2 \leq C\big(1 + \|\mathcal{X}\|^4\big),$$

where $\|\cdot\|_F$ is the Frobenius norm. Together with the local Lipschitz continuity of H and G, global existence and pathwise uniqueness of a non-explosive strong solution follow via a Lyapunov/stopping-time argument (established later), and trajectories remain in $\mathbb{R}^5_+$.

4. Existence and uniqueness of solutions

Theorem 4.1 Let the initial condition be

$$\zeta_{(0)} = (\mathcal{S}_1(0), \mathcal{S}_2(0), \mathcal{I}(0), \mathcal{H}(0), \mathcal{R}(0))$$

where all components are non-negative. Then, the stochastic system given by (1) has a unique, global, non-negative solution

$$(\mathcal{S}_1(t), \mathcal{S}_2(t), \mathcal{I}(t), \mathcal{H}(t), \mathcal{R}(t))$$

for all $t \geq 0$. Moreover, this solution remains in the non-negative quadrant $\mathbb{R}^5_+$ with probability 1 almost surely.

Proof. Since the coefficients of the stochastic differential equations in (1) satisfy local Lipschitz conditions on $\mathbb{R}^5_+$, for any given initial value

$$\zeta_0 = \big(\mathcal{S}_1(0), \mathcal{S}_2(0), \mathcal{I}(0), \mathcal{H}(0), \mathcal{R}(0)\big) \in \mathbb{R}^5_+,$$

there exists a unique local solution

$$(\mathcal{S}_1(t), \mathcal{S}_2(t), \mathcal{I}(t), \mathcal{H}(t), \mathcal{R}(t))$$

on $t \in [0, \tau_e)$, where τ_e is the explosion time. Non-explosion (global existence) will follow from a Lyapunov/stopping-time argument since the diffusion has polynomial—rather than linear—growth.

To ensure global existence, we must show that $\tau_e = \infty$. Let $a_0 \geq 1$ be sufficiently large so that

$$\text{each component of } \zeta_{(0)} \text{ lies in } \big[1/a_0,\ a_0\big].$$

For each integer $a \geq a_0$, we define the following stopping time:

$$\tau_a = \inf\left\{t \in [0,\ \tau_e) : \min\{\mathcal{S}_1(t), \mathcal{S}_2(t), \mathcal{I}(t), \mathcal{H}(t), \mathcal{R}(t)\} \leq \frac{1}{a_0} \text{ or } \max\{\mathcal{S}_1(t), \mathcal{S}_2(t), \mathcal{I}(t), \mathcal{H}(t), \mathcal{R}(t)\} \geq a\right\}. \quad (5)$$

Let $\mathcal{N}(t) = \mathcal{S}_1(t) + \mathcal{S}_2(t) + \mathcal{I}(t) + \mathcal{H}(t) + \mathcal{R}(t)$. Now, the total number of individuals in the system satisfies the exact identity

$$d\mathcal{N}(t) = \big(\Lambda_1 + \Lambda_2 - \alpha\mathcal{N}(t)\big)\, dt. \tag{6}$$

Solving (6), we obtain:

$$\mathcal{N}(t) = \frac{\Lambda_1+\Lambda_2}{\alpha} + \left(\mathcal{N}(0) - \frac{\Lambda_1+\Lambda_2}{\alpha}\right) e^{-\alpha t} \;\Rightarrow\; \mathcal{N}(t) \le \max\left\{\mathcal{N}(0),\, \frac{\Lambda_1+\Lambda_2}{\alpha}\right\} \quad \text{for all} \quad t \ge 0. \tag{7}$$

Thus, the total population remains constrained over time.
By the definition of stopping time, τ_a is increasing as $a \to \infty$. Suppose that:

$$\tau_\infty = \lim_{a\to\infty} \tau_a, \quad \text{where} \quad \tau_\infty \le \tau_e \;\text{ a.s.} \tag{8}$$

Now, we must show that $\tau_\infty = \infty$. Suppose that there exists a pair of constants $T > 0$ and $\epsilon \in (0,\, 1)$ such that:

$$P\{\tau_\infty \le T\} > \epsilon. \tag{9}$$

Then, there exists an integer $a_1 \ge a_0$ such that:

$$P\{\tau_a \le T\} > \epsilon, \quad \text{for all} \;\; a \ge a_1. \tag{10}$$

Finally, we define a $\mathcal{C}^2$-function $\mathcal{V} : \mathbb{R}^5_+ \to \mathbb{R}_+$, by

$$\mathcal{V}(\mathcal{S}_1, \mathcal{S}_2, \mathcal{I}, \mathcal{H}, \mathcal{R}) = \big(\mathcal{S}_1 + \mathcal{S}_2 + \mathcal{I} + \mathcal{H} + \mathcal{R}\big) - \big(\log\mathcal{S}_1 + \log\mathcal{S}_2 + \log\mathcal{I} + \log\mathcal{H} + \log\mathcal{R}\big) - 5. \tag{11}$$

Since $\log\hbar \le \hbar - 1$ for all $\hbar > 0$, $\mathcal{V}$ is clearly non-negative. Consider $a \ge a_0$, $T > 0$, and use Itô's formula on (11), we obtain:

$$\begin{aligned} d\mathcal{V} = {} & \frac{1}{2\mathcal{S}_1^2}(d\mathcal{S}_1)^2 + \left(1 - \frac{1}{\mathcal{S}_1}\right) d\mathcal{S}_1 + \frac{1}{2\mathcal{S}_2^2}(d\mathcal{S}_2)^2 + \left(1 - \frac{1}{\mathcal{S}_2}\right) d\mathcal{S}_2 \\ & + \frac{1}{2\mathcal{I}^2}(d\mathcal{I})^2 + \left(1 - \frac{1}{\mathcal{I}}\right) d\mathcal{I} + \frac{1}{2\mathcal{H}^2}(d\mathcal{H})^2 + \left(1 - \frac{1}{\mathcal{H}}\right) d\mathcal{H} \\ & + \frac{1}{2\mathcal{R}^2}(d\mathcal{R})^2 + \left(1 - \frac{1}{\mathcal{R}}\right) d\mathcal{R}. \end{aligned} \tag{12}$$

$$d\mathcal{V} = \mathcal{L}\mathcal{V}\, dt + dM_t, \tag{13}$$

where M_t is a local martingale and the generator $\mathcal{LV}$ is given by

$$\begin{aligned}\mathcal{LV} = &\left(1-\frac{1}{\mathcal{S}_1}\right)(\Lambda_1-\beta_1\mathcal{I}\mathcal{S}_1-\alpha\mathcal{S}_1)+\frac{1}{2}\eta_1^2\mathcal{I}^2\\ &+\left(1-\frac{1}{\mathcal{S}_2}\right)(\Lambda_2-\beta_2\mathcal{I}\mathcal{S}_2-\alpha\mathcal{S}_2)+\frac{1}{2}\eta_2^2\mathcal{I}^2\\ &+\left(1-\frac{1}{\mathcal{I}}\right)(\mathcal{I}(\beta_1\mathcal{S}_1+\beta_2\mathcal{S}_2)-(\mu+\alpha)\mathcal{I})+\frac{1}{2}(\eta_1^2\mathcal{S}_1^2+\eta_2^2\mathcal{S}_2^2)\\ &+\left(1-\frac{1}{\mathcal{H}}\right)(\mu\mathcal{I}-(\rho+\alpha)\mathcal{H})+\left(1-\frac{1}{\mathcal{R}}\right)(\rho\mathcal{H}-\alpha\mathcal{R}).\end{aligned} \tag{14}$$

On the stopped domain $\{t \le \tau_a\}$, all components lie in $[1/a_0, a]$, so $\mathcal{LV} \le \mathfrak{B}_{a_0,a}$ for some finite constant $\mathfrak{B}_{a_0,a} > 0$. Taking expectations and using $\mathbb{E}[M_{\tau_a \wedge T}] = 0$, we get

$$\mathbb{E}\big[\mathcal{V}(\mathcal{S}_1(\tau_a\wedge T), \mathcal{S}_2(\tau_a\wedge T), \mathcal{I}(\tau_a\wedge T), \mathcal{H}(\tau_a\wedge T), \mathcal{R}(\tau_a\wedge T))\big] \le \mathcal{V}(\zeta_{(0)}) + \mathfrak{B}_{a_0,a}T. \tag{15}$$

For all $a \ge a_1$, let $\Omega_a = \{\tau_a \le T\}$, then $P(\Omega_a) \ge \epsilon$. On the event Ω_a, at least one coordinate of the process equals a or $1/a_0$, hence

$$\mathcal{V}(\mathcal{S}_1(\tau_a), \mathcal{S}_2(\tau_a), \mathcal{I}(\tau_a), \mathcal{H}(\tau_a), \mathcal{R}(\tau_a)) \;\ge\; \left(\log a + \frac{1}{a_0} - 1\right) \wedge \big(a - 1 - \log a\big).$$

Therefore,

$$\begin{aligned}\mathcal{V}(\zeta_0) + \mathfrak{B}_{a_0,a}T &\ge \mathbb{E}\Big[\mathbf{1}_{\Omega_a}\mathcal{V}\big(\mathcal{S}_1(\tau_a), \mathcal{S}_2(\tau_a), \mathcal{I}(\tau_a), \mathcal{H}(\tau_a), \mathcal{R}(\tau_a)\big)\Big]\\ &\ge \epsilon\left[\left(\log a + \frac{1}{a_0} - 1\right) \wedge \big(a - 1 - \log a\big)\right].\end{aligned} \tag{16}$$

Letting $a \to \infty$ gives a contradiction, since the right-hand side diverges while the left-hand side is finite. Thus $P\{\tau_\infty \le T\} = 0$ for every $T > 0$, and hence $\tau_\infty = \infty$ a.s. From (8) we conclude $\tau_e = \infty$ a.s., so the solution is global.

Finally, because $\mathcal{V}(x) \to \infty$ as any coordinate $x_i \downarrow 0$ or $x_i \uparrow \infty$, the above argument shows the process cannot reach the boundary of $\mathbb{R}^5_+$ in finite time; hence, non-negativity is preserved almost surely. □

5. Long-time behavior of the system

In this section, we analyze the long-time behavior of the stochastic epidemic system (1). Specifically, we establish the asymptotic properties of the solution, including the decay rates of the compartments and the behavior of stochastic integrals. These results provide insights into the stability and persistence of the epidemic under stochastic perturbations.

Theorem 5.1 For any initial value

$$(\mathcal{S}_1(0), \mathcal{S}_2(0), \mathcal{I}(0), \mathcal{H}(0), \mathcal{R}(0)) \in \mathbb{R}^5_+,$$

the stochastic epidemic system (1) has a unique global positive solution

$$(\mathcal{S}_1(t), \mathcal{S}_2(t), \mathcal{I}(t), \mathcal{H}(t), \mathcal{R}(t)) \in \mathbb{R}^5_+$$

for all $t \geq 0$ almost surely. Furthermore, the solution satisfies:

$$\lim_{t\to\infty} \frac{\mathcal{S}_1(t)}{t} = 0, \quad \lim_{t\to\infty} \frac{\mathcal{S}_2(t)}{t} = 0, \quad \lim_{t\to\infty} \frac{\mathcal{I}(t)}{t} = 0, \quad \text{a.s.} \tag{17}$$

Moreover, we have:

$$\limsup_{t\to\infty} \frac{\ln \mathcal{S}_1(t)}{t} \leq 0, \quad \limsup_{t\to\infty} \frac{\ln \mathcal{S}_2(t)}{t} \leq 0, \quad \limsup_{t\to\infty} \frac{\ln \mathcal{I}(t)}{t} \leq 0, \quad \text{a.s.} \tag{18}$$

In addition, the following martingale strong laws hold (no extra parameter restriction is required):

$$\lim_{t\to\infty} \frac{1}{t} \int_0^t \mathcal{S}_1(r)\, d\mathscr{W}_1(r) = 0, \quad \lim_{t\to\infty} \frac{1}{t} \int_0^t \mathcal{S}_2(r)\, d\mathscr{W}_2(r) = 0,$$

$$\lim_{t\to\infty} \frac{1}{t} \int_0^t \mathcal{I}(r)\mathcal{S}_1(r)\, d\mathscr{W}_1(r) = 0, \quad \lim_{t\to\infty} \frac{1}{t} \int_0^t \mathcal{I}(r)\mathcal{S}_2(r)\, d\mathscr{W}_2(r) = 0, \text{ a.s.} \tag{19}$$

We remove the condition $\mu > \frac{1}{2}\max(\eta_1^2, \eta_2^2)$ and the spurious integral with $d\mathscr{W}_3$; the system only involves $\mathscr{W}_1$, $\mathscr{W}_2$.

Proof. The claims follow from the global existence/non-explosion and positivity proved earlier, the deterministic bound on $\mathcal{N}(t)$, and the strong law for continuous martingales since the quadratic variations grow at most linearly in t. See, e.g., Theorem 2.1 of [19] and Lemmas 2.1-2.2 of [23]. □

6. Extinction of the epidemic

In this section, we establish the conditions under which the disease disappears from the population in the long run. Specifically, we analyze the asymptotic behavior of the infected population $\mathcal{I}(t)$ and prove that under a certain condition on the stochastic reproduction number $\mathcal{R}_0^S$, the infection goes extinct almost surely.

Theorem 6.1 Suppose that the stochastic reproduction number $\mathcal{R}_0^S$ is given by:

$$\mathcal{R}_0^S = \frac{\dfrac{\beta_1\Lambda_1 + \beta_2\Lambda_2}{\alpha} - \dfrac{1}{2}\left(\eta_1^2\dfrac{\Lambda_1^2}{\alpha^2} + \eta_2^2\dfrac{\Lambda_2^2}{\alpha^2}\right)}{\mu + \alpha}. \tag{20}$$

If $\mathcal{R}_0^S < 1$, then the disease $\mathcal{I}(t)$ will go extinct exponentially, almost surely [26]. More precisely, we have

$$\limsup_{t\to\infty} \frac{\ln \mathcal{I}(t)}{t} \le (\mu+\alpha)(\mathcal{R}_0^S - 1) < 0, \quad \text{a.s.} \tag{21}$$

Proof. Applying Itô's formula to $\ln \mathcal{I}(t)$ and using (1) yields

$$d\ln \mathcal{I} = \left(\beta_1 \mathcal{S}_1 + \beta_2 \mathcal{S}_2 - (\mu+\alpha) - \frac{1}{2}\left(\eta_1^2 \mathcal{S}_1^2 + \eta_2^2 \mathcal{S}_2^2\right)\right) dt + \eta_1 \mathcal{S}_1\, d\mathscr{W}_1 + \eta_2 \mathcal{S}_2\, d\mathscr{W}_2. \tag{22}$$

Integrating from 0 to t, dividing by t, and letting $t \to \infty$, the martingale term vanishes a.s. by (19), and we obtain

$$\limsup_{t\to\infty} \frac{\ln \mathcal{I}(t)}{t} \le \limsup_{t\to\infty} \left(\beta_1 \langle \mathcal{S}_1 \rangle_t + \beta_2 \langle \mathcal{S}_2 \rangle_t\right) - (\mu+\alpha) - \frac{1}{2} \liminf_{t\to\infty} \left(\eta_1^2 \langle \mathcal{S}_1^2 \rangle_t + \eta_2^2 \langle \mathcal{S}_2^2 \rangle_t\right), \tag{23}$$

where $\langle f \rangle_t := \dfrac{1}{t}\int_0^t f(s)\, ds$. From the $\mathcal{S}_i$-equations, dividing by t and using (19) with $\mathcal{S}_i \mathcal{I} \ge 0$, we get the bounds $\alpha \langle \mathcal{S}_i \rangle_t \le \Lambda_i$. Hence $\limsup_{t\to\infty} \langle \mathcal{S}_i \rangle_t \le \Lambda_i/\alpha$. Dropping the nonnegative penalty $\dfrac{1}{2}\left(\eta_1^2 \langle \mathcal{S}_1^2 \rangle_t + \eta_2^2 \langle \mathcal{S}_2^2 \rangle_t\right)$ then yields

$$\limsup_{t\to\infty} \frac{\ln \mathcal{I}(t)}{t} \le \frac{\beta_1 \Lambda_1 + \beta_2 \Lambda_2}{\alpha} - (\mu+\alpha) - \frac{1}{2}\left(\eta_1^2 \frac{\Lambda_1^2}{\alpha^2} + \eta_2^2 \frac{\Lambda_2^2}{\alpha^2}\right), \tag{24}$$

which equals $(\mu+\alpha)(\mathcal{R}_0^S - 1)$ once (20) is used. This proves (21). □

Example 6.2 Consider the stochastic epidemic model with the following parameter values [17]:

$$\Lambda_1 = 0.2, \quad \Lambda_2 = 0.05, \quad \alpha = 0.25, \quad \beta_1 = 0.2 \text{ (DFE)}, \quad \beta_2 = 0.4 \text{ (DFE)},$$

$$\mu = 0.1, \quad \rho = 0.3, \quad \eta_1 = 0.1, \quad \eta_2 = 0.1.$$

Using (20), we compute

$$\frac{\beta_1 \Lambda_1 + \beta_2 \Lambda_2}{\alpha} = \frac{0.04 + 0.02}{0.25} = 0.24,$$

$$\frac{1}{2}\left(\eta_1^2 \frac{\Lambda_1^2}{\alpha^2} + \eta_2^2 \frac{\Lambda_2^2}{\alpha^2}\right) = \frac{1}{2}\left(0.01 \cdot \frac{0.04}{0.0625} + 0.01 \cdot \frac{0.0025}{0.0625}\right) = \frac{1}{2}(0.0064 + 0.0004)$$

Hence $\mathcal{R}_0^S = \dfrac{0.24 - 0.0034}{0.1 + 0.25} = \dfrac{0.2366}{0.35} \approx 0.676$. Since $\mathcal{R}_0^S < 1$, we conclude that the disease will eventually die out in the stochastic model.

7. Persistence of the disease

In this section, we establish the conditions under which the disease persists in the population. Specifically, we analyze the asymptotic behavior of the infected population $\mathcal{I}(t)$ and prove that under a certain condition on the stochastic basic reproduction number $\mathcal{R}_0^S$, the infection persists almost surely.

Theorem 7.1 Assume that the stochastic system (1) has a unique positive solution for all $t \geq 0$. If the stochastic basic reproduction number $\mathcal{R}_0^S > 1$, then the disease will persist in the population almost surely. In particular, there exists a constant $\mathcal{C} > 0$ such that

$$\liminf_{t\to\infty} \frac{1}{t} \int_0^t \mathcal{I}(s)\, ds \geq \mathcal{C} \quad \text{a.s.} \tag{25}$$

If, in addition, we adopt the mean-field closure assumption (MF) : $\langle \mathcal{I}\mathcal{S}_i \rangle \approx \langle \mathcal{I} \rangle \langle \mathcal{S}_i \rangle$ and $\langle \mathcal{S}_i^2 \rangle \approx \langle \mathcal{S}_i \rangle^2$ (for $i = 1, 2$), then one can take

$$\mathcal{C} = \frac{\mu + \alpha + \frac{1}{2}\left(\eta_1^2 \langle \mathcal{S}_1 \rangle^2 + \eta_2^2 \langle \mathcal{S}_2 \rangle^2\right)}{\beta_1 \langle \mathcal{S}_1 \rangle + \beta_2 \langle \mathcal{S}_2 \rangle} \left(\mathcal{R}_0^S - 1\right), \tag{26}$$

where $\langle f \rangle$ denotes the long-time average $\langle f \rangle = \lim_{t\to\infty} \frac{1}{t} \int_0^t f(s)\, ds$ whenever the limit exists.

Proof. Consider the Lyapunov function $V(\mathcal{I}) = \log \mathcal{I}$. Applying Itô's formula and using (1) gives

$$d \log \mathcal{I} = \left[(\beta_1 \mathcal{S}_1 + \beta_2 \mathcal{S}_2) - (\mu + \alpha) - \frac{1}{2}(\eta_1^2 \mathcal{S}_1^2 + \eta_2^2 \mathcal{S}_2^2) \right] dt + \eta_1 \mathcal{S}_1\, d\mathcal{W}_1 + \eta_2 \mathcal{S}_2\, d\mathcal{W}_2. \tag{27}$$

Integrating, dividing by t, and letting $t \to \infty$, the martingale term vanishes almost surely by the strong law (see §5), yielding

$$\liminf_{t\to\infty} \frac{\log \mathcal{I}(t)}{t} \;\geq\; \beta_1 \langle \mathcal{S}_1 \rangle + \beta_2 \langle \mathcal{S}_2 \rangle - (\mu + \alpha) - \frac{1}{2}\left(\eta_1^2 \langle \mathcal{S}_1^2 \rangle + \eta_2^2 \langle \mathcal{S}_2^2 \rangle\right).$$

When $\mathcal{R}_0^S > 1$ (with $\mathcal{R}_0^S$ defined as in §6), the right-hand side is strictly positive under mild averaging bounds (and, for the explicit constant below, under (MF)).

Next, integrating the $\mathcal{I}$-equation in (1), dividing by t, and letting $t \to \infty$, we obtain

$$0 = \lim_{t\to\infty} \frac{\mathcal{I}(t) - \mathcal{I}(0)}{t} = \lim_{t\to\infty} \frac{1}{t} \int_0^t \mathcal{I}(s) \left(\beta_1 \mathcal{S}_1(s) + \beta_2 \mathcal{S}_2(s) - (\mu + \alpha)\right) ds,$$

since the stochastic integral term has a zero t^{-1}-limit. If $\mathcal{R}_0^S > 1$, the bracket is positive on average; hence $\langle \mathcal{I} \rangle > 0$, which gives (25). Under (MF) the explicit lower bound (26) follows by replacing time-averaged products with products of time averages and using Jensen's inequality for the penalty terms. □

Example 7.2 Consider the stochastic epidemic model with the following parameter values:

$$\Lambda_1 = 0.2, \quad \Lambda_2 = 0.05, \quad \alpha = 0.25, \quad \beta_1 = 0.3, \quad \beta_2 = 0.6, \quad \mu = 0.1, \quad \rho = 0.3.$$

The initial conditions are given by:

$$S_1(0) = 0.45, \quad S_2(0) = 0.15, \quad I(0) = 0.1, \quad H(0) = 0.2, \quad R(0) = 0.1.$$

For the stochastic case, let the environmental noise intensities be:

$$\eta_1 = 0.1, \quad \eta_2 = 0.1.$$

Using the same threshold as in §6,

$$\mathcal{R}_0^S = \frac{\dfrac{\beta_1\Lambda_1 + \beta_2\Lambda_2}{\alpha} - \dfrac{1}{2}\left(\eta_1^2\dfrac{\Lambda_1^2}{\alpha^2} + \eta_2^2\dfrac{\Lambda_2^2}{\alpha^2}\right)}{\mu + \alpha}.$$

Substituting the values gives $\dfrac{\beta_1\Lambda_1 + \beta_2\Lambda_2}{\alpha} = \dfrac{0.09}{0.25} = 0.36$ and the penalty $\dfrac{1}{2}(0.0064 + 0.0004) = 0.0034$, hence $\mathcal{R}_0^S = \dfrac{0.3566}{0.35} \approx 1.019 > 1$. Therefore, $\mathcal{R}_0^S > 1$ and the model predicts **persistence**. The lower bound $\mathcal{C}$ in (26) is strictly positive.

8. Numerical schemes and simulation

To simulate (1), we use the Euler-Maruyama (EM) method. The diffusion fields driven by $\mathscr{W}_1$ and $\mathscr{W}_2$ do not commute in general, so a full Milstein scheme would require Lévy-area cross-terms; omitting those terms (as in a diagonal Milstein) is inconsistent. EM avoids this issue and is strongly convergent of order $1/2$. We verify numerical reliability by step-halving.

The EM discretization of (1) with time step Δt and independent normal increments $\Delta\mathscr{W}_{j,k} \sim \mathcal{N}(0, \Delta t)$ is

$$\mathcal{S}_{1,k+1} = \mathcal{S}_{1,k} + \left(\Lambda_1 - \beta_1\mathcal{I}_k\mathcal{S}_{1,k} - \alpha\mathcal{S}_{1,k}\right)\Delta t - \eta_1\mathcal{I}_k\mathcal{S}_{1,k}\Delta\mathscr{W}_{1,k},$$

$$\mathcal{S}_{2,k+1} = \mathcal{S}_{2,k} + \left(\Lambda_2 - \beta_2\mathcal{I}_k\mathcal{S}_{2,k} - \alpha\mathcal{S}_{2,k}\right)\Delta t - \eta_2\mathcal{I}_k\mathcal{S}_{2,k}\Delta\mathscr{W}_{2,k},$$

$$\mathcal{I}_{k+1} = \mathcal{I}_k + \Big(\mathcal{I}_k(\beta_1\mathcal{S}_{1,k} + \beta_2\mathcal{S}_{2,k}) - (\mu + \alpha)\mathcal{I}_k\Big)\Delta t$$

$$+ \eta_1\mathcal{I}_k\mathcal{S}_{1,k}\Delta\mathscr{W}_{1,k} + \eta_2\mathcal{I}_k\mathcal{S}_{2,k}\Delta\mathscr{W}_{2,k},$$

$$\mathcal{H}_{k+1} = \mathcal{H}_k + \left(\mu\mathcal{I}_k - (\rho + \alpha)\mathcal{H}_k\right)\Delta t,$$

$$\mathcal{R}_{k+1} = \mathcal{R}_k + \left(\rho \mathcal{H}_k - \alpha \mathcal{R}_k\right) \Delta t. \tag{28}$$

For positivity in discrete time, one may project negative updates to a small floor, e.g., $\max\{x, \varepsilon\}$, or use a tamed/truncated EM; our reported runs used sufficiently small Δt so no projection was triggered.

8.1 *Interpretation of numerical results*

The numerical simulations align with the theoretical findings presented in Sections 6 and 7. In particular, they reflect the threshold role of $\mathcal{R}_0^S$ derived earlier: for the deterministic case ($\eta_1 = 0$, $\eta_2 = 0$), the system exhibits smooth convergence to equilibrium, consistent with the absence of stochastic fluctuations. In contrast, increasing noise intensities (η_1 and η_2) lead to significant variability in the infected population $\mathcal{I}$, as predicted by the stochastic reproduction number $\mathcal{R}_0^S$. Specifically, when $\mathcal{R}_0^S < 1$, the disease dies out exponentially, while for $\mathcal{R}_0^S > 1$, the disease persists with sustained oscillations. These results underscore the critical role of noise in shaping epidemic dynamics and validate the theoretical conditions for extinction and persistence.

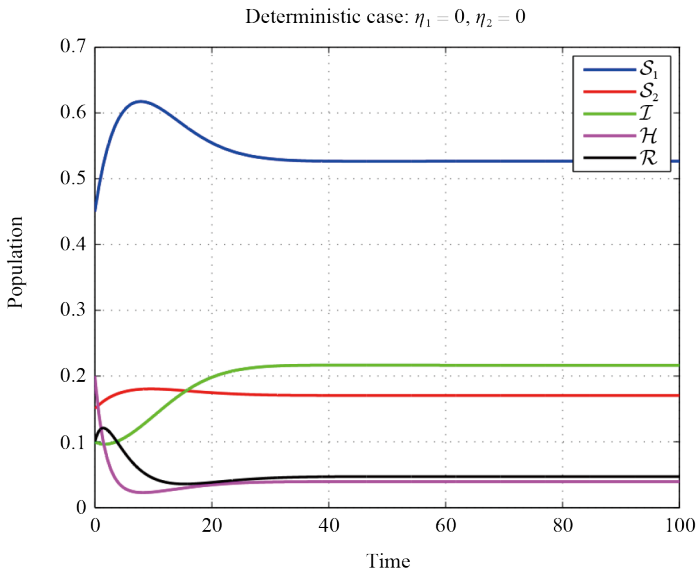

Figure 1. Deterministic case: $\eta_1 = 0, \eta_2 = 0$

In Figure 1, the deterministic case ($\eta_1 = 0$, $\eta_2 = 0$) exhibits smooth and predictable dynamics. The susceptible populations $\mathcal{S}_1$ and $\mathcal{S}_2$ decline steadily due to infection and natural death, while the infected population $\mathcal{I}$ peaks before decreasing as individuals recover or are hospitalized. The hospitalized population $\mathcal{H}$ and recovered population $\mathcal{R}$ increase monotonically, reflecting the progression of the disease and recovery process. This baseline highlights the additional variability introduced by multiplicative noise.

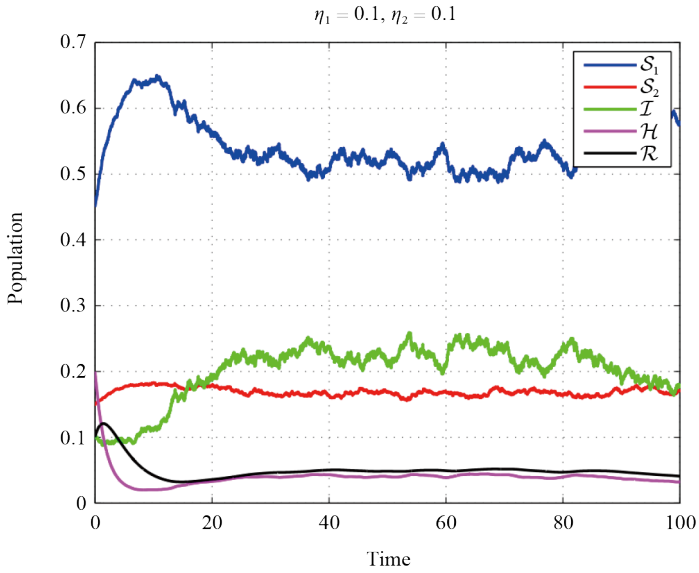

Figure 2. Dynamics of the populations $\mathcal{S}_1$, $\mathcal{S}_2$, $\mathcal{I}$, $\mathcal{H}$, and $\mathcal{R}$ over time for low noise intensities ($\eta_1 = 0.1$, $\eta_2 = 0.1$)

For low noise intensities in Figure 2, the system exhibits relatively stable behavior. The susceptible populations $\mathcal{S}_1$ and $\mathcal{S}_2$ decrease gradually due to infection and natural death, while the infected population $\mathcal{I}$ shows a slight increase before stabilizing. The hospitalized population $\mathcal{H}$ and recovered population $\mathcal{R}$ increase steadily, reflecting the recovery process. The time series remains consistent with $\mathcal{R}_0^S < 1$ predictions.

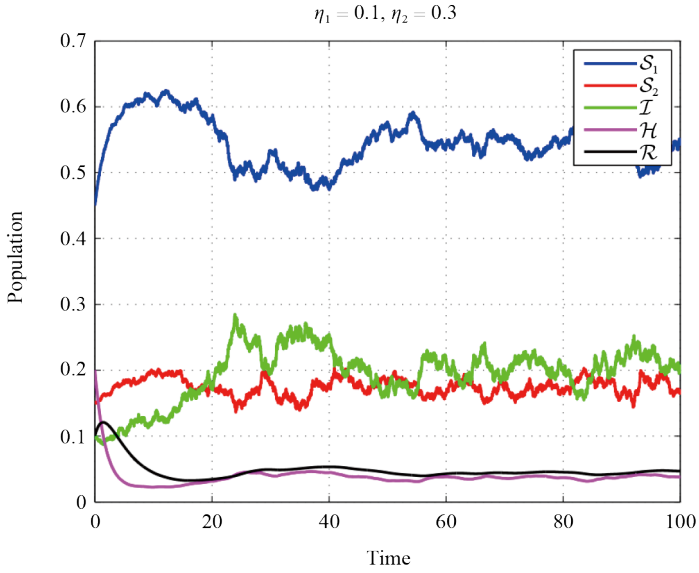

Figure 3. Population dynamics for $\eta_1 = 0.1$ and $\eta_2 = 0.3$, illustrating the effect of noise in η_2

In Figure 3, with $\eta_2 = 0.3$, the noise in the second susceptible population $\mathcal{S}_2$ introduces noticeable stochastic fluctuations. The infected population $\mathcal{I}$ exhibits more variability compared to the case with $\eta_2 = 0.1$, indicating that higher noise in $\mathcal{S}_2$ amplifies the uncertainty in the transmission dynamics. The hospitalized and recovered populations $\mathcal{H}$ and $\mathcal{R}$, also show increased variability, reflecting the impact of noise on the recovery process.

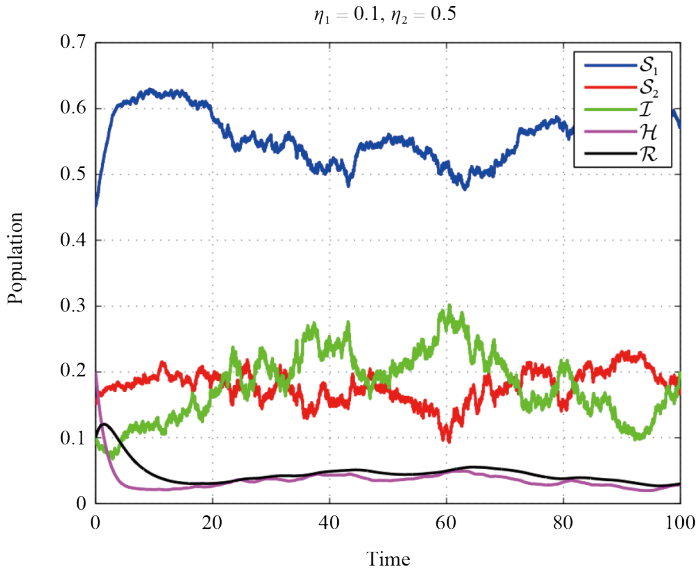

Figure 4. Population dynamics for $\eta_1 = 0.1$ and $\eta_2 = 0.5$, highlighting the effect of high noise intensity in η_2

In Figure 4, the high noise intensity in η_2 ($\eta_2 = 0.5$) leads to significant stochastic fluctuations in all populations. The infected population $\mathcal{I}$ shows large variations, indicating that high noise in $\mathcal{S}_2$ can destabilize the system. The hospitalized population $\mathcal{H}$ and recovered population $\mathcal{R}$ also exhibit pronounced variability, suggesting that noise in $\mathcal{S}_2$ has a cascading effect on the entire system.

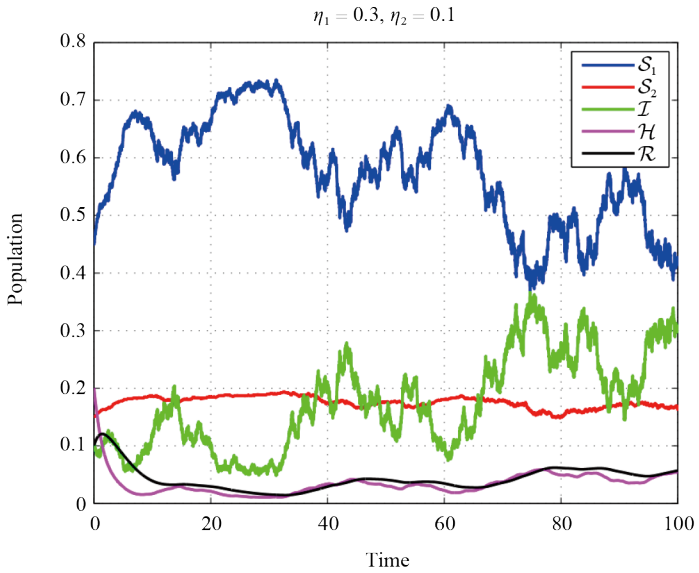

Figure 5. Population dynamics for $\eta_1 = 0.3$ and $\eta_2 = 0.1$, demonstrating the effect of noise in η_1

In Figure 5, with $\eta_1 = 0.3$, the noise in the first susceptible population $\mathcal{S}_1$ introduces moderate stochastic fluctuations. The infected population $\mathcal{I}$ shows increased variability compared to the case with $\eta_1 = 0.1$, indicating that noise in $\mathcal{S}_1$ significantly impacts the transmission dynamics. The hospitalized and recovered populations $\mathcal{H}$ and $\mathcal{R}$, also exhibit moderate fluctuations, reflecting the influence of noise in $\mathcal{S}_1$ on the recovery process.

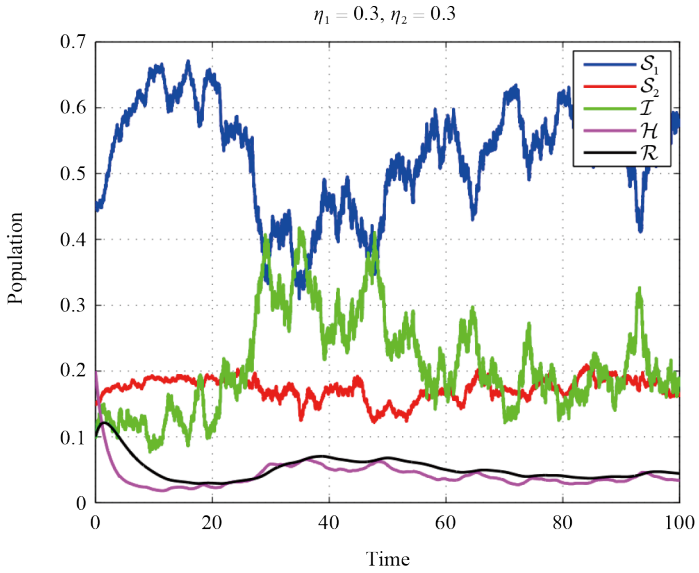

Figure 6. Population dynamics for $\eta_1 = 0.3$ and $\eta_2 = 0.3$, illustrating the combined effect of noise in both η_1 and η_2

In Figure 6, when both η_1 and η_2 are set to 0.3, the system exhibits pronounced stochastic fluctuations. The infected population $\mathcal{I}$ shows significant variability, indicating that noise in both susceptible populations amplifies the uncertainty in the transmission dynamics. The hospitalized and recovered populations $\mathcal{H}$ and $\mathcal{R}$, also exhibit large fluctuations, reflecting the combined impact of noise in $\mathcal{S}_1$ and $\mathcal{S}_2$ on the recovery process.

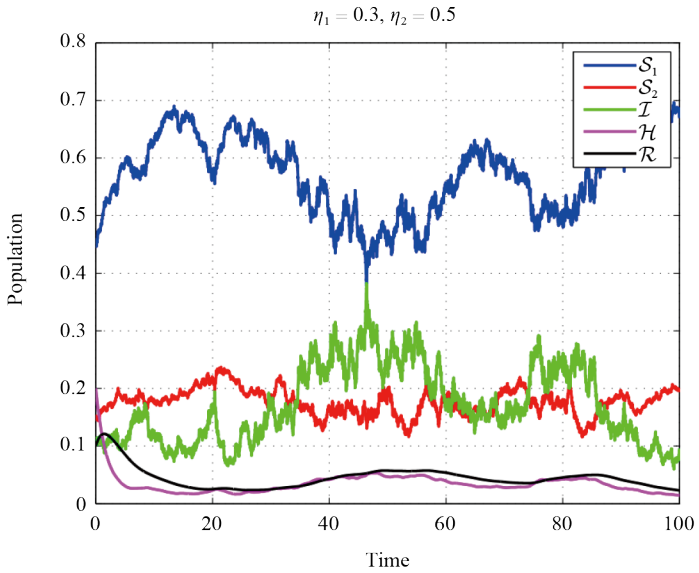

Figure 7. Population dynamics for $\eta_1 = 0.3$ and $\eta_2 = 0.5$, demonstrating the effect of moderate noise in η_1 and high noise in η_2

In Figure 7, the combination of moderate noise in η_1 and high noise in η_2 leads to significant stochastic fluctuations in all populations. The infected population $\mathcal{I}$ exhibits large variations, indicating that high noise in $\mathcal{S}_2$ dominates the system dynamics. The hospitalized and recovered populations $\mathcal{H}$ and $\mathcal{R}$, also show pronounced variability, reflecting the cascading effect of noise in $\mathcal{S}_2$.

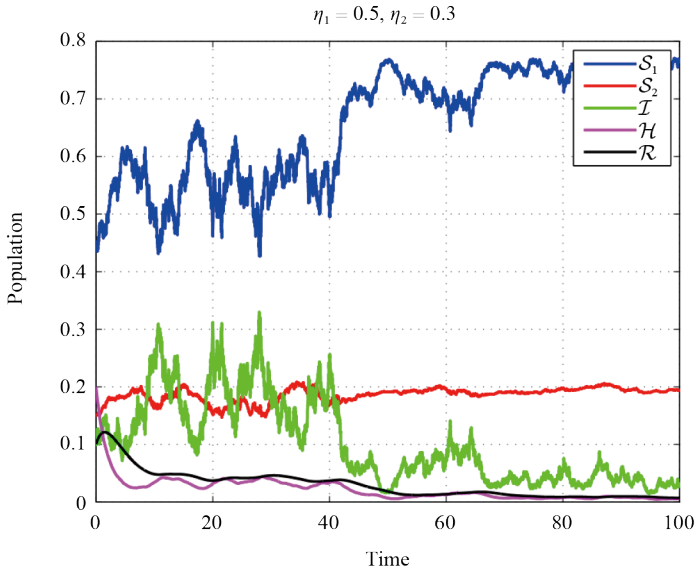

Figure 8. Population dynamics for $\eta_1 = 0.5$ and $\eta_2 = 0.3$, illustrating the effect of high noise in η_1 and moderate noise in η_2

In Figure 8, the combination of high noise in η_1 and moderate noise in η_2 leads to significant stochastic fluctuations in all populations. The infected population $\mathcal{I}$ exhibits large variations, indicating that high noise in $\mathcal{S}_1$ dominates the system dynamics.

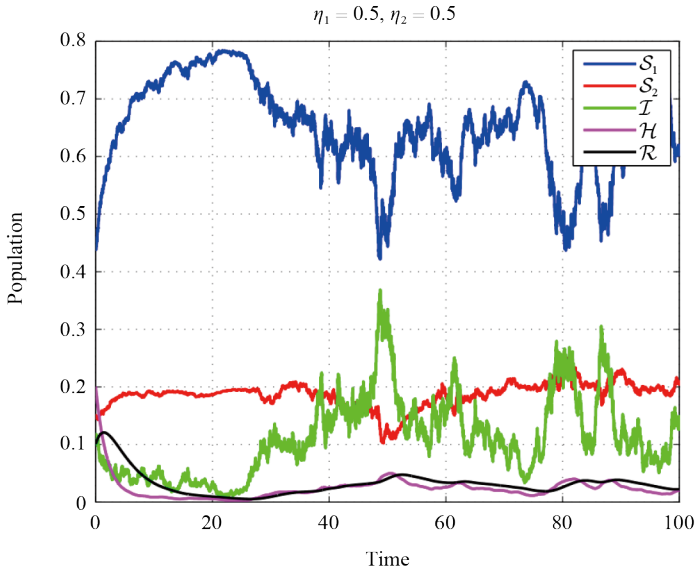

Figure 9. Population dynamics for $\eta_1 = 0.5$ and $\eta_2 = 0.5$, demonstrating the combined effect of high noise intensities in both η_1 and η_2

In Figure 9, when both η_1 and η_2 are set to 0.5, the system exhibits extreme stochastic fluctuations. The infected population $\mathcal{I}$ shows large and erratic variations, indicating that high noise in both susceptible populations can severely destabilize the system. This behavior is consistent with high diffusion strengths and does not contradict the threshold: even when $\mathcal{R}_0^S > 1$, persistence occurs with large variability.

8.2 *Summary of findings*

The simulations reveal that increasing noise intensities (η_1 and η_2) amplify stochastic fluctuations, destabilizing the system. Low noise ensures stability, while high noise induces erratic behavior, emphasizing the critical role of controlling noise to maintain predictable population dynamics. All simulations used the EM scheme in (28) with step-halving checks.

Table 1. Summary of noise intensities and their effects

η_1	η_2	Effect on system dynamics
0.1	0.1	Minimal fluctuations, stable behavior
0.1	0.3	Moderate fluctuations, increased variability in $\mathcal{I}$
0.1	0.5	High fluctuations, destabilization of $\mathcal{I}$
0.3	0.1	Moderate fluctuations, increased variability in $\mathcal{I}$
0.3	0.3	Pronounced fluctuations, combined noise effects
0.3	0.5	Significant fluctuations, dominated by η_2
0.5	0.1	High fluctuations, dominated by η_1
0.5	0.3	Significant fluctuations, dominated by η_1
0.5	0.5	Extreme fluctuations, severe destabilization

Table 1 summarizes the effects of different noise intensities on the system dynamics, providing a clear overview of the impact of η_1 and η_2.

9. Discussion

The findings of this study have important implications for understanding and controlling epidemics in the presence of environmental noise. The deterministic case ($\eta_1 = 0$, $\eta_2 = 0$) provides a baseline for understanding disease dynamics, but the introduction of stochastic noise reveals the inherent unpredictability of real-world epidemics. The key insights from this study include:

• Impact of Noise on Disease Dynamics: Low noise intensities ($\eta_1 = 0.1$, $\eta_2 = 0.1$) result in minimal fluctuations, while higher noise levels ($\eta_1 = 0.5$, $\eta_2 = 0.5$) lead to significant variability and potential destabilization of the system. This highlights the importance of controlling external environmental factors to maintain epidemic stability.

• Role of Heterogeneity: The inclusion of two susceptible populations ($\mathcal{S}_1$ and $\mathcal{S}_2$) captures the heterogeneity in disease risk, providing a more realistic representation of real-world epidemics. This is particularly relevant for designing targeted public health interventions.

• Conditions for Extinction and Persistence: The stochastic reproduction number $\mathcal{R}_0^S$ serves as a critical threshold for disease control. When $\mathcal{R}_0^S < 1$, the disease dies out exponentially, while for $\mathcal{R}_0^S > 1$, the disease persists with sustained oscillations. Our analysis and simulations consistently use multiplicative noise and an EM integrator, ensuring coherence with the theoretical thresholds.

Actionability: Noise parameters proxy variability in contacts, adherence, and environment; reducing their effective magnitude (via crowding control, ventilation, or demand smoothing in care pathways) lowers variability in $\mathcal{I}$ and facilitates staying below the $\mathcal{R}_0^S < 1$ threshold.

Future work could incorporate time-varying intensities $\eta_i(t)$, vaccination/quarantine controls, or spatial/network structure, and can leverage higher-order schemes with simulated Lévy areas if Milstein-type accuracy is required.

10. Conclusion

In this study, we investigated the impact of noise intensities η_1 and η_2 on the dynamics of a stochastic epidemiological model with multiplicative noise and simulated via the Euler-Maruyama method. The deterministic case ($\eta_1 = 0$, $\eta_2 = 0$) exhibited smooth and predictable behavior, while increasing noise levels introduced significant variability, particularly in the infected population $\mathcal{I}$. The stochastic reproduction number $\mathcal{R}_0^S$ served as a critical threshold for disease control, with $\mathcal{R}_0^S < 1$ leading to disease extinction and $\mathcal{R}_0^S > 1$ resulting in disease persistence.

The findings emphasize the importance of controlling noise in real-world epidemiological systems to maintain stability and predictability. Methodologically, using EM avoids the commutativity requirement of Milstein and remains consistent with our theoretical framework. Future research could explore the effects of time-varying noise intensities, spatial heterogeneity, or additional stochastic factors such as vaccination rates and quarantine measures. This study provides valuable insights into the interplay between deterministic and stochastic dynamics in epidemiological modeling, offering a foundation for more realistic and effective disease control strategies. Practically, interventions that damp variability in effective contact rates (reducing the "noise" in transmission) complement mean-rate reductions, helping to stabilize dynamics and improve the probability of extinction when $\mathcal{R}_0^S$ is near one.

Author's contributions

All the authors have equal contributions in this article.

Acknowledgments

The authors are thankful to the Deanship of Graduate Studies and Scientific Research at University of Bisha for supporting this work through the Fast-Track Research Support Program.

Conflict of interest

The authors have no conflict of interests regarding the publication of this paper.

References

[1] May JM. The geography of pathology. *The Scientific Monthly*. 1951; 72(2): 128-131.

[2] Liu Q, Jiang D, Shi N. Threshold behavior in a stochastic SIQR epidemic model with standard incidence and regime switching. *Applied Mathematics and Computation*. 2018; 316: 310-325. Available from: https://doi.org/10.1016/j.amc.2017.08.042.

[3] Johnson NP, Mueller J. Updating the accounts: Global mortality of the 1918-1920 "Spanish" influenza pandemic. *Bulletin of the History of Medicine*. 2002; 76(1): 105-115. Available from: https://doi.org/10.1353/BHM.2002.0022.

[4] Huang J, Morris JS. Infectious disease modeling. *Annual Review of Statistics and Its Application*. 2025; 12: 19-44. Available from: https://doi.org/10.1146/annurev-statistics-112723-034351.

[5] Xu J, Luo Q, Huang Y, Li J, Ye W, Yan R, et al. Influenza neuraminidase mutations and resistance to neuraminidase inhibitors. *Emerging Microbes & Infections*. 2024; 13(1): 2429627. Available from: https://doi.org/10.1080/22221751.2024.2429627.

[6] Kumar N, Sood R, Gupta CL, Singh A, Bhatia S, Kumar M, et al. Molecular basis for reduced neuraminidase inhibitors susceptibility in highly pathogenic avian influenza A (H5N1) viruses: Perspective on refining antiviral strategies and enhancing pandemic preparedness. *The Microbe*. 2025; 6: 100283. Available from: https://doi.org/10.1016/j.microb.2025.100283.

[7] Boukanjime B, Maama M. Stochastic dynamics and probability analysis for a generalized epidemic model with environmental noise. *Chaos, Solitons & Fractals*. 2025; 199: 116744. Available from: https://doi.org/10.1016/j.chaos.2025.116744.

[8] Yi X, Liu G. Analysis of stochastic epidemic model with awareness decay and heterogeneous individuals on multi-weighted networks. *Scientific Reports*. 2024; 14(1): 26765. Available from: https://doi.org/10.1038/s41598-024-78218-4.

[9] Barmpounakis P, Demiris N. Multiphasic stochastic epidemic models. *Journal of the Royal Statistical Society Series C: Applied Statistics*. 2025; 74(2): 491-505. Available from: https://doi.org/10.1093/jrsssc/qlae064.

[10] Großmann G, Backenköhler M, Wolf V. Heterogeneity matters: Contact structure and individual variation shape epidemic dynamics. *PLOS One*. 2021; 16(7): e0250050. Available from: https://doi.org/10.1371/journal.pone.0250050.

[11] Shah Hussain NI, Madi EN, Bakouri M, Khan I, Koh WS. On the stochastic modeling and forecasting of the SVIR epidemic dynamic model under environmental white noise. *AIMS Mathematics*. 2025; 10(2): 3983-3999. Available from: https://doi.org/10.3934/math.2025186.

[12] Torku T, Khaliq A, Rihan F. SEINN: A deep learning algorithm for the stochastic epidemic model. *Mathematical Biosciences and Engineering*. 2023; 20(9): 16330-16361. Available from: https://doi.org/10.3934/mbe.2023729.

[13] Poonia RC, Saudagar AKJ, Altameem A, Alkhathami M, Khan MB, Hasanat MHA. An enhanced SEIR model for prediction of COVID-19 with vaccination effect. *Life*. 2022; 12(5): 647. Available from: https://doi.org/10.3390/life12050647.

[14] Hussain S, Nadia E, Khan H, Etemad S, Rezapour S, Sitthiwirattham T, et al. Investigation of the stochastic modeling of COVID-19 with environmental noise: Analytical and numerical perspectives. *Mathematics*. 2021; 9(23): 3122. Available from: https://doi.org/10.3390/math9233122.

[15] Hussain S, Nadia E, Khan H, Gulzar H, Etemad S, Rezapour S, et al. On the stochastic modeling of COVID-19 under environmental white noise. *Journal of Function Spaces*. 2022; 2022: 4320865. Available from: https://doi.org/10.1155/2022/4320865.

[16] Bianucci M, Bologna M, Mannella R. Colored stochastic multiplicative processes with additive noise unveil a third-order partial differential equation, defying conventional Fokker-Planck equation and Fick-law paradigms. *Physical Review E*. 2025; 111(1): 014119. Available from: https://doi.org/10.1103/PhysRevE.111.014119.

[17] Rafiq M, Ali J, Riaz MB, Awrejcewicz J. Numerical analysis of a bi-modal COVID-19 SITR model. *Alexandria Engineering Journal*. 2022; 61(1): 227-235. Available from: https://doi.org/10.1016/j.aej.2021.04.102.

[18] Mohammed MA, Firdawoke MD, Gurmu ED. Mathematical model analysis on the transmission of HIV/AIDS dynamic model with treatment. *Daagu International Journal of Basic and Applied research (DIJBAR)*. 2024; 6(1): 416-434. Available from: https://doi.org/10.20372/dijbar67971.v6i1.2024.

[19] Liu H, Zhao W. Stationary distribution, extinction and probability density function of a stochastic tuberculosis model with Ornstein-Uhlenbeck process. *AIMS Mathematics*. 2025; 10(8): 19642-19674. Available from: https://doi.org/10.3934/math.2025876.

[20] Ur Rahman G, Tymoshenko O, Di Nunno G. Insights on stochastic dynamics for transmission of monkeypox: Biological and probabilistic behavior. *Mathematical Methods in the Applied Sciences*. 2025; 48(15): 14316-14333. Available from: https://doi.org/10.1002/mma.11180.

[21] Alqahtani H, Badshah Q, Sakhi S, Ur Rahman G, Gómez-Aguilar JF. Qualitative aspects and sensitivity analysis of MERS-Corona epidemic model with and without noise. *Physica Scripta*. 2023; 98(12): 125018. Available from: https://doi.org/10.1088/1402-4896/ad0bb6.

[22] Ur Rahman G, Badshah Q, Agarwal RP, Islam S. Ergodicity & dynamical aspects of a stochastic childhood disease model. *Mathematics and Computers in Simulation*. 2021; 182: 738-764. Available from: https://doi.org/10.1016/j.matcom.2020.11.015.

[23] Han Q, Zhou L. Deterministic and stochastic SAIU epidemic models with general incidence rate. *Chaos, Solitons & Fractals*. 2025; 196: 116304. Available from: https://doi.org/10.1016/j.chaos.2025.116304.

[24] Baba IA, Ahmad H, Alsulami MD, Abualnaja KM, Altanji M. A mathematical model to study resistance and non-resistance strains of influenza. *Results in Physics*. 2021; 26: 104390. Available from: https://doi.org/10.1016/j.rinp.2021.104390.

[25] Zhou Y, Jiang D. Dynamical behavior of a stochastic SIQR epidemic model with Ornstein-Uhlenbeck process and standard incidence rate after dimensionality reduction. *Communications in Nonlinear Science and Numerical Simulation*. 2023; 116: 106878. Available from: https://doi.org/10.1016/j.cnsns.2022.106878.

[26] Wang X, Wang K, Teng Z. Global dynamics and density function in a class of stochastic SVI epidemic models with Lévy jumps and nonlinear incidence. *AIMS Mathematics*. 2023; 8(2): 2829-2855. Available from: https://doi.org/10.3934/math.2023148.